

TU-566
hep-ph/9905486

R_b and R_ℓ in MSSM without R-Parity

Jin Min Yang*

Department of Physics, Tohoku University, Aoba-ku, Sendai 980-8578, Japan

Abstract

We examined $Z\ell^+\ell^-$ and $Zb\bar{b}$ couplings in the minimal supersymmetric model (MSSM) with explicit R -parity violating interactions. We found the top quark L-violating couplings λ'_{i3k} and B-violating couplings λ''_{3j3} could give significant contributions through the top quark loops. To accomodate the latest R_ℓ data, λ'_{i3k} are sujept to stringent bounds, some of which can be much stronger than the current bounds. Within the current perturbative unitarity bound of 1.25 for λ''_{3j3} , the R_b value in R -violating MSSM agrees well with the experimental data at 2σ level, but may lie outside the 1σ range depending on the involved sfermion mass.

Typeset using REVTeX

*Address after March of 2000: Institute of Theoretical Physics, Academia Sinica, Beijing, China

I. INTRODUCTION

The Standard Model (SM) has been very successful phenomenologically. Despite its success, the SM is still believed to be a theory effective at the electroweak scale and that some new physics must exist at higher energy regimes. So far there have been numerous speculations on the possible forms of new physics beyond the SM. In the effective Lagrangian approach [1], the observable effects of new physics at the SM energy scale are described in the form of anomalous interactions. Among the various candidates for new physics which have predictive power at energies not far above the weak scale, the most intensively studied one is the weak-scale minimal supersymmetric model (MSSM) [2], which has many attractive features and is often arguably the most promising one.

In the MSSM, the invariance of R -parity, defined by $R = (-1)^{2S+3B+L}$ for a field with spin S , baryon-number B and lepton-number L , is often imposed on the Lagrangian in order to maintain the separate conservation of baryon-number and lepton-number. However, this conservation is not dictated by any fundamental principle such as gauge invariance and there is no compelling theoretical motivation for it. The most general superpotential of the MSSM consistent with the $SU(3) \times SU(2) \times U(1)$ symmetry and supersymmetry contains R -violating interactions which are given by [3]

$$\mathcal{W}_R = \frac{1}{2} \lambda_{ijk} L_i L_j E_k^c + \lambda'_{ijk} L_i Q_j D_k^c + \frac{1}{2} \lambda''_{ijk} \epsilon^{abd} U_{ia}^c D_{jb}^c D_{kd}^c + \mu_i L_i H_2, \quad (1.1)$$

where $L_i(Q_i)$ and $E_i(U_i, D_i)$ are the left-handed lepton (quark) doublet and right-handed lepton (quark) singlet chiral superfields. i, j, k are generation indices and c denotes charge conjugation. a, b and d are the color indices and ϵ^{abd} is the total antisymmetric tensor. $H_{1,2}$ are the Higgs-doublets chiral superfields. The λ_{ijk} and λ'_{ijk} are L -violating couplings, λ''_{ijk} B -violating couplings. λ_{ijk} is antisymmetric in the first two indices and λ''_{ijk} is antisymmetric in the last two indices. The phenomenological studies for these R -violating couplings were started long time ago [3]. While this is an interesting problem in its own right, the recent anomalous events at HERA [4] and the evidence of neutrino oscillation [5] might provide an additional motivation for the study of these R -violating couplings. So both theorists and experimentalists have recently intensively examined the phenomenology of R -parity breaking supersymmetry in various processes [6,7] and obtained some bounds [8].

It is notable that some of these R -violating couplings contribute to the precisely measured $Zb\bar{b}$ and $Z\ell^+\ell^-$ couplings through sfermion-fermion loops. Since the MSSM is a renormalizable field theory and the sparticles get their masses through explicit soft breaking terms, the decoupling theorem [9] implies that the effects of these sparticle loops will be suppressed by some orders of $1/M_{SUSY}$ and vanish as M_{SUSY} goes far above the weak scale. So, in general, these sfermion-fermion loop effects on lower energy observables are small. However, due to the non-decoupling property of heavy SM particles (which get masses through spontaneous gauge symmetry breaking), the effects of the sfermion-fermion loops with the fermion being the top quark (hereafter called the top quark loops) may be enhanced by the large top quark mass. Therefore, the R -violating top quark couplings in Eq.(1.1), λ'_{i3k} and λ''_{3jk} , which currently subject to quite weak bounds (see Ref. [8] for a review), may give rise to significant contributions through the top quark loops.

Although some bounds on the R -violating couplings were derived from $R_\ell \equiv \Gamma(Z \rightarrow \text{hadrons})/\Gamma(Z \rightarrow \ell^+\ell^-)$ a few years ago [10], it is necessary to give a thorough examination

for the R -violating quantum effects on $Zb\bar{b}$ and $Z\ell^+\ell^-$ couplings since the measurements of both $R_b \equiv \Gamma(Z \rightarrow b\bar{b})/\Gamma(Z \rightarrow \text{hadrons})$ and R_ℓ have been much improved nowadays [11,12]. Also, when deriving bounds from R_b and R_ℓ , the R -conserving MSSM quantum effects, which were neglected in previous studies [10], should be included. In this paper we study the contributions of the trilinear explicit R -violating interactions to $Zb\bar{b}$ and $Z\ell^+\ell^-$ couplings. By using the latest data of R_b and R_ℓ , we examine the bounds on the top quark R -violating couplings. The R -conserving MSSM quantum effects on $Zb\bar{b}$ vertex are also taken into account in our analyses.

Note that at the level of the superpotential, the explicit L -violating terms $\mu_i L_i H_2$ can be rotated away by a field redefinition [3]. However, such a redefinition does not leave the full Lagrangian invariant when including the soft-breaking terms [13]. We in this paper focus on the trilinear explicit R -violating interactions and ignore the effects of the terms $\mu_i L_i H_2$ or the so-called spontaneous R -violation induced by the non-zero VEVs of sneutrinos.

This paper is organized as follows. In Sec. II we calculate the contributions of R -violating MSSM to $Zb\bar{b}$ and $Z\ell^+\ell^-$ couplings. In Sec. III we present the contributions to R_b and R_ℓ , and derive the limits from the latest experimental data. Finally, we give the conclusion in Sec. IV.

II. $ZB\bar{B}$ AND $Z\ell^+\ell^-$ IN R -VIOLATING MSSM

Neglecting the dipole-moment coupling which are suppressed by m_b/m_Z , the R -violating MSSM contribution to $Zb\bar{b}$ vertex takes the form

$$\Delta V_{Zb\bar{b}} = i \frac{e}{s_W c_W} \gamma_\mu \left[P_R g_R^b \Delta_R^b + P_L g_L^b \Delta_L^b \right], \quad (2.1)$$

where $P_{R,L} = (1 \pm \gamma_5)/2$ and g_L^b (g_R^b) is the $Zb_L\bar{b}_L$ ($Zb_R\bar{b}_R$) coupling in the SM. (Throughout this paper the subscripts R and L stand for chirality.) The new physics contribution factors Δ_L^b and Δ_R^b comprise of both the R -conserving MSSM contribution and R -violating contribution which are denoted by

$$\Delta_L^b = \Delta_L^{(\text{MSSM})} + \Delta_L^{(R)}, \quad (2.2)$$

$$\Delta_R^b = \Delta_R^{(\text{MSSM})} + \Delta_R^{(R)}. \quad (2.3)$$

The R -conserving MSSM interactions contribute to R_b mainly through [14]:

- (1) Chargino-stop loops. Their contribution is most likely sizable since they contain the large $\tilde{t}_R - b_L$ -Higgsino Yukawa coupling squared, which is proportional to $\frac{M_t^2}{M_W^2}(1 + \cot^2 \beta)$.
- (2) Charged and neutral Higgs loops. For a very light CP-odd Higgs boson A^0 ($50 \sim 80$ GeV) and very large $\tan \beta$ (~ 50), their contribution could be sizable [14].
- (3) Neutralino-sbottom loops. Their contribution is negligibly small for low and intermediate $\tan \beta$, but could be sizable for very large $\tan \beta$ [14].

Since the dominant MSSM contribution is from the chargino-stop loops for low and intermediate $\tan\beta$ ($1 \sim 30$), we in our calculation consider the chargino-stop loops while give a brief comment on the effects of other loops. A detailed calculation of the full one-loop effects of MSSM on $Zb\bar{b}$ coupling can be found in [14]. Here we present the results for the chargino loops. The Feynman diagrams for chargino-stop loops are shown in Fig.1. The contribution factor $\Delta_R^{(\text{MSSM})} \equiv \Delta_R^{(\tilde{t}_L)}$ arise from the first three diagrams of Fig.1 induced by $\tilde{t}_L - b_R - \tilde{\chi}_j^+$ Yukawa couplings, while $\Delta_L^{(\text{MSSM})} \equiv \Delta_L^{(\tilde{t}_L)} + \Delta_L^{(\tilde{t}_R)}$ with $\Delta_L^{(\tilde{t}_L)}$ arising from the middle three diagrams of Fig.1 induced by $\tilde{t}_L - b_L - \tilde{\chi}_j^+$ gauge couplings and $\Delta_L^{(\tilde{t}_R)}$ from the last three diagrams of Fig.1 induced by $\tilde{t}_R - b_L - \tilde{\chi}_j^+$ Yukawa couplings. The expressions of $\Delta_R^{(\tilde{t}_L)}$, $\Delta_L^{(\tilde{t}_L)}$ and $\Delta_L^{(\tilde{t}_R)}$ are presented in the Appendix.

Through loop diagrams, the R -violating couplings λ''_{ij3} and λ'_{ij3} contribute to $Zb_R\bar{b}_R$, and λ'_{i3k} contribute to $Zb_L\bar{b}_L$. (Note that, for example, λ''_{ij3} can also induce $Zb_L\bar{b}_L$ coupling through loops, which is suppressed by M_b^2/M_Z^2 and thus negligibly small.) The Feynman diagrams for the loop contributions of these couplings to $Zb\bar{b}$ coupling are shown in Figs.2, 3 and 4, respectively. Their contributions denoted as $\Delta_R^{(\lambda''_{ij3})}$, $\Delta_R^{(\lambda'_{ij3})}$, and $\Delta_L^{(\lambda'_{i3k})}$ are presented in the Appendix.

Through loops, the couplings λ_{ijk} and λ'_{ijk} with $i = 1, 2$ and 3 contribute to $Z\ell^+\ell^-$ with $\ell = e, \mu$ and τ , respectively. The pure leptonic couplings λ_{ijk} are not relevant to the top quark and will not be considered in our analyses. The Feynman diagrams of the contribution of λ'_{ijk} to $Z\ell_L^-\ell_L^+$ are shown in Fig.5. (The loops of λ'_{ijk} can also induce $Z\ell_R^-\ell_R^+$ coupling, which is suppressed by M_ℓ^2/M_Z^2 and thus negligibly small.) The contribution to $Z\ell^+\ell^-$ vertex takes the form

$$\Delta V_{Z\ell^+\ell^-} = i \frac{e}{s_W c_W} \gamma_\mu \left[P_R g_R^\ell \Delta_R^\ell + P_L g_L^\ell \Delta_L^\ell \right], \quad (2.4)$$

where g_L^ℓ and g_R^ℓ are the couplings in the SM, and Δ_L^ℓ and Δ_R^ℓ the contributions from the couplings λ'_{ijk} with $\Delta_R^\ell \approx 0$ and Δ_L^ℓ being obtained from $\Delta_L^{(\lambda'_{i3k})}$ with substitutions of $b \rightarrow \ell$, $\nu^i \rightarrow u^j$ and $\tilde{\nu}^i \rightarrow \tilde{u}^j$.

We would like to make a few comments on the above calculations:

- (a) In our calculations, we used dimensional regularization to control the ultraviolet divergences in the virtual loop corrections and we adopted the on-mass-shell renormalization scheme. The ultraviolet divergences in the self-energy and the vertex loops are contained in Feynman integrals. We have checked that in our results, the ultraviolet divergences cancelled as a result of renormalizability of the MSSM.
- (b) In our calculations, various sfermion states are involved. We note that in general there exist the mixing between left- and right-handed sfermions of each flavor (denoted as \tilde{f}_L and \tilde{f}_R), as suggested by low-energy supergravity models [15]. (We do not consider the flavor mixing of sfermions.) So \tilde{f}_L and \tilde{f}_R are in general not the physical states (mass eigenstates), instead they are related to mass eigenstates \tilde{f}_1 and \tilde{f}_2 by a unitary rotation:

$$\tilde{f}_R = \cos\theta \tilde{f}_1 - \sin\theta \tilde{f}_2, \quad (2.5)$$

$$\tilde{f}_L = \sin\theta \tilde{f}_1 + \cos\theta \tilde{f}_2. \quad (2.6)$$

In our calculations, we give the results in terms of \tilde{f}_L and \tilde{f}_R , which can be easily applied to the general case by using the above relations between $\tilde{f}_{L,R}$ and $\tilde{f}_{1,2}$.

- (c) We neglected the R -conserving MSSM contribution to $Z\ell^+\ell^-$ couplings because they are expected to be small, unlike the $Zb\bar{b}$ case where chargino-stop loops could contribute significantly.
- (d) While it is theoretically possible to have both B -violating and L -violating terms in the Lagrangian, the non-observation of proton decay imposes very stringent conditions on their simultaneous presence. In our calculation (and in the following numerical calculations) we consider the presence of one non-zero coupling at one time.

Let us neglect the mixing between the left- and right-handed sfermions of each flavor, and assume the value of 100 GeV for all sparticles and find out which coupling could give large contribution. (For heavier sparticles the contribution becomes smaller.) The top quark mass is fixed to 175 GeV throughout the paper. The results are found to be

$$\text{Fig.2 : } \Delta_R^b / |\lambda_{ij3}''|^2 = \begin{cases} -5.62\% & \text{for } \lambda_{3j3}'' \\ 0.183\% & \text{for } \lambda_{1j3}'' , \lambda_{2j3}'' \end{cases} \quad (2.7)$$

$$\text{Fig.3 : } \Delta_R^b / |\lambda_{ij3}'|^2 = \begin{cases} -2.76\% & \text{for } \lambda_{i33}' \\ 0.184\% & \text{for } \lambda_{i13}' , \lambda_{i23}' \end{cases} \quad (2.8)$$

$$\text{Fig.4 : } \Delta_L^b / |\lambda_{i3k}'|^2 = 0.09\% \quad (2.9)$$

$$\text{Fig.5 : } \Delta_L^\ell / |\lambda_{ijk}'|^2 = \begin{cases} -0.77\% & \text{for } \lambda_{i3k}' \\ 0.09\% & \text{for } \lambda_{i1k}' , \lambda_{i2k}' \end{cases} \quad (2.10)$$

As expected, even for the same magnitudes of the coupling strength, the top quark interactions contribute more significantly than others, i.e., λ_{3j3}'' and λ_{i33}' contribute more significantly to $Zb_R\bar{b}_R$, while λ_{i3k}' to $Z\ell_L^-\ell_L^+$. In each case, the dominant contribution is found to arise from the top quark loops.

As for the contribution from R -conserving MSSM, for comparison, we assume $\theta_t = 0$ (i.e., $M_{\tilde{t}_R} = M_{\tilde{t}_1}$ and $M_{\tilde{t}_L} = M_{\tilde{t}_2}$), and the masses of both stops take the value of 100 GeV. Assuming $M = 250$ GeV and $\mu = -100$ GeV, then for $\tan\beta = 1$ (30), the contributions are found to be

$$\Delta_R^{(\tilde{t}_L)} = -0.001\% \quad (-0.28\%) \quad (2.11)$$

$$\Delta_L^{(\tilde{t}_L)} = -0.03\% \quad (-0.02\%) \quad (2.12)$$

$$\Delta_L^{(\tilde{t}_R)} = 0.27\% \quad (0.17\%) \quad (2.13)$$

As expected, $\Delta_L^{(\tilde{t}_R)}$ is large because it is proportional to $\frac{M_t^2}{M_W^2}(1 + \cot^2\beta)$. For large $\tan\beta$, $\Delta_R^{(\tilde{t}_L)}$ also becomes sizable because it is enhanced by the factor $\frac{M_b^2}{M_W^2}(1 + \tan^2\beta)$. $\Delta_L^{(\tilde{t}_L)}$ arise from the gauge coupling and is found to be always small. We realize that although the magnitude of $\Delta_R^{(\tilde{t}_L)}$ becomes comparable to that of $\Delta_L^{(\tilde{t}_R)}$ for large $\tan\beta$, its contribution to R_b is suppressed by the factor $(g_R^b/g_L^b)^2 \approx 1/30$ relative to the contribution of $\Delta_L^{(\tilde{t}_R)}$. So, for low and intermediate $\tan\beta$, the MSSM contribution is dominated by the last three diagrams of Fig.1, which are induced by the $\tilde{t}_R - b_L - \text{Higgsino Yukawa coupling}$. Since the sign of $\Delta_R^{(\tilde{t}_L)}$

is opposite to that of $\Delta_L^{(\tilde{t}_R)}$, the MSSM contribution to R_b is relatively large when \tilde{t}_R is the lighter stop \tilde{t}_1 ($\theta_t = 0$), $\tan\beta$ takes the small value and the lighter chargino is Higgsino-like.

Comparing Eqs.(2.7,2.8) with Eqs.(2.13), we find that for $|\lambda'| \approx 1$ or $|\lambda''| \approx 1$ the R -violating contribution to R_b is of comparable magnitude to the MSSM contribution. (Here again we note the fact that the contribution of Δ_R^b to R_b is suppressed by the factor $(g_R^b/g_L^b)^2 \approx 1/30$ relative to the contribution of Δ_L^b .) If the stops are significantly lighter than other sfermions which appear in the top quark loops of R -violating contributions, the MSSM contribution to R_b can be more sizable. So the MSSM contributions should be considered when deriving the bounds on R -violating couplings from R_b .

III. R_B AND R_ℓ IN R -VIOLATING MSSM

From the results of the preceding section, we found that the contributions of R -violating top quark interactions to both $Zb\bar{b}$ and $Z\ell^+\ell^-$ could be significant, with the dominant contributions arising from the top quark loops. The magnitudes of the contributions are proportional to the relevant coupling strength squared.

For the L -violating top quark couplings λ'_{i3k} , only λ'_{131} , λ'_{231} and λ'_{133} are already strongly constrained by atomic parity violation, ν_μ deep-inelastic scattering and ν_e -mass [8], respectively. In the case of the B -violating top quark couplings λ''_{3j3} , none of them have been well constrained by other processes. Some theoretical bounds on λ''_{3j3} can be derived under specific assumptions. The constraint of perturbative unitarity at the SUSY breaking scale M_{SUSY} would require all the couplings $|\lambda''|^2/(4\pi) < 1$, i.e., $|\lambda''| < 3.54$. A stronger bound can be obtained if we assume the gauge group unification at $M_U = 2 \times 10^{16}$ GeV and the Yukawa couplings Y_t , Y_b and Y_τ to remain in the perturbative domain in the whole range up to M_U . They imply $Y_i(\mu) < 1$ for $\mu < 2 \times 10^{16}$ GeV. Then we obtain an upper bound of 1.25 for all λ'' [16]. So it is likely for these top quark R -violating couplings, subject to the current limits, cause large effects on R_b and/or R_ℓ and, as a result, their current bounds could be improved further.

In the following we present some representative results. For simplicity, we again neglect the mixing between the left- and right-handed sfermion states for each flavor, and further assume the mass degeneracy for all sfermions. (We will comment on the mixing effects of stops or sbottoms later.) For the parameters M and μ in the chargino sector, we take two representative scenarios: $M = 250$ GeV and $\mu = -100$ GeV (Higgsino-like), and $M = 100$ GeV and $\mu = -250$ GeV (gaugino-like). In the above two scenarios, the lighter chargino mass is 112 GeV for $\tan\beta = 2$ and 92 GeV for $\tan\beta = 30$. (Note that the lower bound of 91 GeV on the chargino mass was obtained from the LEP runs at c.m. energy of 183 GeV [18].)

A. R_b in MSSM with λ''_{3j3}

The coupling λ''_{3j3} ($j = 1$ or 2) contributes to both $Z \rightarrow b\bar{b}$ through the $t - \tilde{d}_R^j$ loops and $Z \rightarrow d^j\bar{d}^j$ through $t - \tilde{b}_R$ loops. If we assume the mass degeneracy between \tilde{b}_R and \tilde{d}_R^j , and neglect the masses of the final quark states, then the contribution to R_b is given by

$$\Delta R_b = 2(1 - \xi R_b^{SM}) R_b^{SM} \frac{\Delta_L^b + (g_R^b/g_L^b)^2 \Delta_R^b}{1 + (g_R^b/g_L^b)^2}, \quad (3.1)$$

where $\xi = 2$, $\Delta_L^b \approx 0$ and $\Delta_R^b = \Delta_R^{(\lambda''_{3j3})}$ given in the Appendix. The MSSM contribution to R_b is given by Eq.(3.1) with $\xi = 1$ since only $Z \rightarrow b\bar{b}$ in the hadronic decays of Z could get sizable contribution.

We found $\Delta R_b^{(\text{MSSM})}$ is positive and $\Delta R_b^{(\lambda''_{3j3})}$ is negative. The combined contribution ΔR_b is negative for λ''_{3j3} being of $\mathcal{O}(1)$. In Fig.6 we fix $\lambda''_{3j3} = 1.25$ and plot $-\Delta R_b$ as a function of sfermion mass. The limits shown in Fig.6 are from the experimental data and the SM value [11]

$$R_b^{exp} = 0.21642 \pm 0.00073, \quad R_b^{SM} = 0.2158 \pm 0.0002. \quad (3.2)$$

The magnitude of ΔR_b in scenario A (Higgsino-like) is relatively small because this scenario gives the relatively large destructive contribution $\Delta R_b^{(\text{MSSM})}$. As shown in Fig.6, ΔR_b lies within the 2σ range, but goes outside the 1σ range for light sfermion mass. So the perturbative unitarity bound of 1.25 on λ''_{3j3} cannot be improved at 2σ level, but can be improved at 1σ level. The limits on λ''_{3j3} are listed in Table I.

Note that the coupling λ'_{i33} only contributes to $Z \rightarrow b\bar{b}$, and, therefore, the corresponding contribution to R_b is given by Eq.(3.1) with $\xi = 1$, and $\Delta_L^b = \Delta_L^{(\lambda'_{i33})}$ and $\Delta_R^b = \Delta_R^{(\lambda'_{i33})}$ given in the Appendix. In this case, there exist both Δ_R^b , induced dominantly from $t - \tilde{e}_L^i$ loops in Fig.3, and Δ_L^b , induced from $b - \tilde{\nu}_L^i$ and $\tilde{b}_R - \nu^i$ loops in Fig.4. As shown in Eqs.(2.8,2.9), if the masses of \tilde{e}_L^i , $\tilde{\nu}_L^i$ and \tilde{b}_R are the same (or at least not very different), Δ_L^b is relatively small compared with Δ_R^b because the loops in Fig.4 do not involve the top quark. However, the contribution of Δ_L^b to R_b is of comparable magnitude to that of Δ_R^b due to the suppression factor $(g_R^b/g_L^b)^2 \approx 1/30$ for the latter. Since the two contributions have the opposite sign, they cancel to a large extent and, therefore, lead to negligibly small contribution to R_b .

B. R_ℓ in MSSM with λ''_{3j3}

The MSSM corrections contribute to R_ℓ through their effects on $Z \rightarrow b\bar{b}$, which is given by

$$\Delta R_\ell = \xi R_b^{SM} R_\ell^{SM} \frac{\Delta_L^b + (g_R^b/g_L^b)^2 \Delta_R^b}{1 + (g_R^b/g_L^b)^2}, \quad (3.3)$$

with $\xi = 2$, $\Delta_L^b = \Delta_L^{(\tilde{t}_L)} + \Delta_L^{(\tilde{t}_R)}$ and $\Delta_R^b = \Delta_R^{(\tilde{t}_L)}$ given in the Appendix.

The coupling λ''_{3j3} contributes to R_ℓ through its effects on $Z \rightarrow b\bar{b}$ and $Z \rightarrow d^j \bar{d}^j$, which is given by Eq.(3.3) with $\xi = 4$ under the assumption that sfermions involved in the relevant loops have the same mass. (Note that under the same assumption, the bounds on λ''_{3j3} from R_ℓ also apply to λ''_{3jk} which contributes to $Z \rightarrow d^k \bar{d}^k$ and $Z \rightarrow d^j \bar{d}^j$.) Since λ''_{3j3} do not directly couple to any leptonic flavor, we assume leptonic universality in R_ℓ in this case.

We found $\Delta R_\ell^{(\text{MSSM})}$ is positive and $\Delta R_\ell^{(\lambda''_{3j3})}$ is negative. For λ''_{3j3} being of $\mathcal{O}(1)$, the combined contribution ΔR_ℓ is negative. In Fig.7 we fix $\lambda''_{3j3} = 1.25$ and plot $-\Delta R_\ell$ as a

function of sfermion mass. The upper limits in Fig.7 are obtained from the experimental data [11]

$$R_\ell^{\text{exp}} = 20.768 \pm 0.024, \quad R_\ell^{\text{SM}} = 20.748. \quad (3.4)$$

From Fig.7 we see that if λ''_{3j3} takes the largest value allowed by perturbative unitarity, the magnitude of ΔR_ℓ lies outside the 1σ range for sfermion mass less than 1 TeV and outside the 2σ range for sfermion mass less than about 200 GeV. So the perturbative unitarity bounds on λ''_{3j3} can be improved, as listed in Table II.

C. R_ℓ in MSSM with λ'_{i3k}

The coupling λ'_{i33} contributes to R_{ℓ_i} , ($\ell_i = e, \mu$ and τ for $i = 1, 2$ and 3 , respectively) through their effects on $Z \rightarrow \ell_i^- \ell_i^+$ and $Z \rightarrow b\bar{b}$, which is given by

$$\Delta R_{\ell_i} = 2R_{\ell_i}^{\text{SM}} \left[R_b^{\text{SM}} \frac{\Delta_L^b + (g_R^b/g_L^b)^2 \Delta_R^b}{1 + (g_R^b/g_L^b)^2} - \frac{\Delta_{\ell_i}^b + (g_R^e/g_L^e)^2 \Delta_R^b}{1 + (g_R^e/g_L^e)^2} \right]. \quad (3.5)$$

Under the assumption that sfermions involved have the same mass, the effects of λ'_{i33} is the same as λ'_{i3k} which contributes to $Z \rightarrow \ell_i^- \ell_i^+$ and $Z \rightarrow d^k \bar{d}^k$. The R -conserving MSSM contribution to each R_{ℓ_i} can be obtained from Eq.(3.3) by the obvious substitution $\ell \rightarrow \ell_i$.

We found both $\Delta R_{\ell_i}^{(\text{MSSM})}$ and $\Delta R_{\ell_i}^{(\lambda'_{i3k})}$ are positive. For sfermion mass of 200 GeV, the combined contribution ΔR_{ℓ_i} versus λ'_{i3k} is plotted in Figs.8, 9 and 10 for $i = 1, 2$ and 3 , respectively. The magnitude of each ΔR_{ℓ_i} in scenario A (Higgsino-like) is relatively large because this scenario gives the relatively large constructive contribution $\Delta R_{\ell_i}^{(\text{MSSM})}$. The limits plotted in Figs.8-10 are obtained from experimental data and the SM values [11]

$$R_e^{\text{exp}} = 20.803 \pm 0.049, \quad R_e^{\text{SM}} = 20.748 \pm 0.019, \quad (3.6)$$

$$R_\mu^{\text{exp}} = 20.786 \pm 0.033, \quad R_\mu^{\text{SM}} = 20.749 \pm 0.019, \quad (3.7)$$

$$R_\tau^{\text{exp}} = 20.764 \pm 0.045, \quad R_\tau^{\text{SM}} = 20.794 \pm 0.019. \quad (3.8)$$

From Figs.8-10 we see that the contribution in each case may lie outside the 2σ range, depending on the coupling strength. The limits on λ''_{13k} , λ''_{23k} and λ''_{33k} are listed in Tables III, IV and V, respectively.

IV. DISCUSSIONS AND CONCLUSION

A few remarks are due regarding the numerical results:

- (1) The R -conserving MSSM effects are not negligible in deriving the bounds on the R -violating couplings. For example, for sfermion mass of 100 GeV, the 1σ bounds with (without) the MSSM effects are

$$|\lambda_{3j3}''| < 1.07(0.55) \quad (\text{from } R_b), \quad (4.1)$$

$$|\lambda_{3j3}''| < 0.65(0.35) \quad (\text{from } R_\ell), \quad (4.2)$$

$$|\lambda_{13k}'| < 0.73(0.77) \quad (\text{from } R_e), \quad (4.3)$$

$$|\lambda_{23k}'| < 0.60(0.64) \quad (\text{from } R_\mu), \quad (4.4)$$

$$|\lambda_{33k}'| < 0.22(0.32) \quad (\text{from } R_\tau), \quad (4.5)$$

where $\tan \beta = 2$, and $M = 100$ GeV and $\mu = -250$ GeV.

- (2) We note that the limits are not very sensitive to $\tan \beta$ in the range of $\tan \beta > 1$. This is because the R -conserving MSSM effects are dominated by the $\tilde{t}_R - b_L$ -Higgsino Yukawa coupling squared $\sim \frac{M_t^2}{M_W^2}(1 + \cot^2 \beta)$ which is not sensitive to $\tan \beta$ in the range of intermediate and large $\tan \beta$. (Of course, the MSSM effects also have a mild dependence on $\tan \beta$ through chargino masses and the unitary matrice diagonalising the chargino mass matrix.) It is obvious that as $\tan \beta$ goes lower than 1 (which is disfavored by the existing experimental data), the MSSM effects will be greatly enhanced and thus the results will be very sensitive to $\tan \beta$.
- (3) For the MSSM contribution to $Zb\bar{b}$ vertex, we only considered the most important part, i.e., the chargino-stop loops. Since the chargino-stop loops contain the large $\tilde{t}_R - b_L$ -Higgsino Yukawa coupling squared, which is proportional to $\frac{M_t^2}{M_W^2}(1 + \cot^2 \beta)$, they are the dominant MSSM effects in a large part of SUSY parameter space, typically with low or intermediate $\tan \beta$ ($1 \sim 30$). For a very light CP-odd Higgs boson A^0 ($50 \sim 80$ GeV) and very large $\tan \beta$ (~ 50), the Higgs loops may give rise to sizable effects. For very large $\tan \beta$ and light sbottoms, the contribution from the neutralino-sbottom loops may also be sizable. In both cases, the contributions to R_b are positive (adds to the effects of chargino-stop loops), and therefore, the bounds will get weaker for λ_{3j3}'' and stronger for λ_{i3k}' .
- (4) We would like to elaborate again on the effects of sfermion mixings. In our numerical calculations, we neglected the mixing between the left- and right-handed sfermion states for each flavor, and further assume the mass degeneracy for all sfermions. This might be a good approximation for all sfermions except stops and sbottoms, because the mixing is proportional to the corresponding fermion mass [15]. The non-diagonal element is give by [15] $M_{LR} = m_t(\mu \cot \beta + A_t)$ for stop mass matrix and $M_{LR} = m_b(\mu \tan \beta + A_b)$, with A_t and A_b being the coefficients of the trilinear soft SUSY-breaking terms $\tilde{t}_L \tilde{t}_R H_2$ and $\tilde{b}_L \tilde{b}_R H_1$, respectively. So in general the stop mixing is significant and sbottom mixing can also be significant for large $\tan \beta$. This implies that the lighter stop (\tilde{t}_1) or/and the lighter sbottom (\tilde{b}_1) could be significantly lighter than other sfermions¹. The stop \tilde{t}_1 is involved in Fig.1 and the sbottom \tilde{b}_1 is involved in

¹For the lighter stop, the direct search from all four experiments at LEP give a lower mass bound of 75 GeV [17]. The D0 collaboration at FNAL searched for the jets plus \cancel{E}_T signal of stop and obtained the lower mass limit of 90 GeV [19]. However, we should note these bounds may not be

Fig.5 with $k = 3$. So if the lighter stop is significantly lighter than other sfermions, the MSSM contributions from Fig.1 will be more significant and thus the limits get weaker for λ''_{3j3} and stronger for λ'_{i3k} ; if the lighter sbottom is significantly lighter than other sfermions (e.g., in case of very large $\tan\beta$), the couplings λ'_{i3k} will have larger effects on $Z\ell^+\ell^-$ vertex and thus subject to even stronger bounds. The numerical results we presented correspond to the special case $A_t = -\mu \cot\beta$ ($\theta_t = 0$) and $A_b = -\mu \tan\beta$ ($\theta_b = 0$).

- (5) In our numerical calculation we worked in the general MSSM, where the SUSY parameters are arbitrary at the weak scale and thus we have the full parameter space freedom. We note that there are some other popular frameworks called the constrained MSSM models, in which the MSSM is usually embedded in some grand unification scenarios. In such frameworks, there are only a few free parameters at the grand unification scale and all the parameters at the weak scale are generated through the renormalization group equations. We did not consider such models in our analyses.
- (6) In our analyses we evaluated R_b and did not present the calculation for $b\bar{b}$ forward-backward asymmetry A_b . The experimental value of A_b shows a 2.7σ deviation from the SM prediction [11]. To accomodate both A_b and R_b data, the new physics contribution has to shift the left- and right-handed $Zb\bar{b}$ couplings by $\sim -1\%$ and $\sim 30\%$, respectively [12]. While the contribution of -1% might easily be interpreted as a new physics quantum loop correction, as shown by our calculation in R -violating MSSM, a large shift of 30% for right-handed coupling seems too strange to explain. For this reason, it is believed the anomaly of A_b stems from a statistical or systematic effect. From our results we see that although the couplings λ''_{ij3} and λ'_{ij3} contribute to right-handed $Zb\bar{b}$ coupling, they cannot provide an explanation for A_b because their contributions are negative.

In summary, we evaluated the quantum effects of the trilinear R -parity violating interactions on $Z\ell^+\ell^-$ and $Zb\bar{b}$ couplings in the MSSM. We found the top quark R -violating couplings could give significant contributions to $Z\ell^+\ell^-$ and $Zb\bar{b}$ through the top quark loops. We calculated (1) R_b value in the MSSM with λ''_{3j3} ; (2) R_ℓ value in the MSSM with λ''_{3j3} ; (3) R_{ℓ_i} values in the MSSM with λ'_{i3k} ($i = 1, 2, 3$). We found that within the current perturbative unitarity bound of 1.25 for λ''_{3j3} , the R_b value agrees well with the experimental data at 2σ level, but may lie outside the 1σ range for light the involved sfermion mass. The R_ℓ data constrained λ''_{3j3} more severely than R_b data. To accomodate the R_ℓ ($\ell = e, \mu, \tau$) data, λ'_{i3k} are sujct to stringent bounds. A summary of updated current bounds on all R -violating top quark Yukawa couplings are given in Table VI for slepton mass and squark mass of 100 GeV. (Here the squark mass of 100 GeV is chosen just for illustration and for the convinience of comparison with other bounds.) Since the bounds from R_ℓ depend slightly on other SUSY parameters of the MSSM, we took the most conservative bounds from our results.

applicable to the R -violating MSSM since the LSP is no longer stable and thus the basic SUSY signal is no longer the missing energy.

ACKNOWLEDGMENTS

The author thanks Ken-ichi Hikasa for useful discussions. The work is supported in part by the Grant-in-Aid for Scientific Research (No. 10640243) and Grant-in-Aid for JSPS Fellows (No. 97317) from the Japan Ministry of Education, Science, Sports, and Culture.

APPENDIX

The contribution factor $\Delta_R^{(\tilde{t}_L)}$ arise from the first three diagrams of Fig1, $\Delta_L^{(\tilde{t}_L)}$ from the middle three diagrams of Fig.1 and $\Delta_L^{(\tilde{t}_R)}$ from the last three diagrams of Fig.1, which are given by

$$\begin{aligned} \Delta_R^{(\tilde{t}_L)} = & -\frac{g^2}{16\pi^2} \left(\frac{M_b}{\sqrt{2}M_W \cos \beta} \right)^2 \left\{ -|U_{j2}|^2 B_1(M_b, M_{\tilde{\chi}_j}, M_{\tilde{t}_L}) \right. \\ & + U_{j2}^* U_{i2} \frac{O'_{ij}^R}{g_R^b} \left[0.5 - 2C_{24} - M_Z^2(C_{11} - C_{12} + C_{21} - C_{23}) \right. \\ & \left. \left. + \frac{O'_{ij}^L}{O'_{ij}^R} M_{\tilde{\chi}_j}^2 C_0 \right] (k, -p_{\bar{b}}, M_{\tilde{\chi}_j}, M_{\tilde{\chi}_j}, M_{\tilde{t}_L}) \right. \\ & \left. - \frac{g_L^t}{g_R^b} |U_{j2}|^2 2C_{24}(p_b, -k, M_{\tilde{\chi}_j}, M_{\tilde{t}_L}, M_{\tilde{t}_L}) \right\}, \end{aligned} \quad (4.6)$$

$$\begin{aligned} \Delta_L^{(\tilde{t}_L)} = & -\frac{g^2}{16\pi^2} \left\{ -|V_{j1}|^2 B_1(M_b, M_{\tilde{\chi}_j}, M_{\tilde{t}_L}) \right. \\ & + V_{j1} V_{i1}^* \frac{O'_{ij}^L}{g_L^b} \left[0.5 - 2C_{24} - M_Z^2(C_{11} - C_{12} + C_{21} - C_{23}) \right. \\ & \left. + \frac{O'_{ij}^R}{O'_{ij}^L} M_{\tilde{\chi}_j}^2 C_0 \right] (k, -p_{\bar{b}}, M_{\tilde{\chi}_j}, M_{\tilde{\chi}_j}, M_{\tilde{t}_L}) \\ & \left. - \frac{g_L^t}{g_R^b} |V_{j1}|^2 2C_{24}(p_b, -k, M_{\tilde{\chi}_j}, M_{\tilde{t}_L}, M_{\tilde{t}_L}) \right\}, \end{aligned} \quad (4.7)$$

$$\begin{aligned} \Delta_L^{(\tilde{t}_R)} = & -\frac{g^2}{16\pi^2} \left(\frac{M_t}{\sqrt{2}M_W \sin \beta} \right)^2 \left\{ -|V_{j2}|^2 B_1(M_b, M_{\tilde{\chi}_j}, M_{\tilde{t}_R}) \right. \\ & + V_{j2} V_{i2}^* \frac{O'_{ij}^L}{g_L^b} \left[0.5 - 2C_{24} - M_Z^2(C_{11} - C_{12} + C_{21} - C_{23}) \right. \\ & \left. + \frac{O'_{ij}^R}{O'_{ij}^L} M_{\tilde{\chi}_j}^2 C_0 \right] (k, -p_{\bar{b}}, M_{\tilde{\chi}_j}, M_{\tilde{\chi}_j}, M_{\tilde{t}_R}) \\ & \left. - \frac{g_R^t}{g_R^b} |V_{j2}|^2 2C_{24}(p_b, -k, M_{\tilde{\chi}_j}, M_{\tilde{t}_R}, M_{\tilde{t}_R}) \right\}. \end{aligned} \quad (4.8)$$

Here the functions B_1 and C_{ij} , C_0 are 2- and 3-point Feynman integrals defined in [20], and their functional dependences are indicated in the bracket following them with k , p_b and $p_{\bar{b}}$ being the momentum of Z -boson, b and \bar{b} , respectively. The O'_{ij}^L and O'_{ij}^R are defined by $O'_{ij}^L = -V_{i1} V_{j1}^* - V_{i2} V_{j2}^*/2 + \delta_{ij} \sin^2 \theta_W$ and $O'_{ij}^R = -U_{i1}^* U_{j1} - U_{i2}^* U_{j2}/2 + \delta_{ij} \sin^2 \theta_W$,

respectively. The unitary matrix elements U_{ij} and V_{ij} , and the chargino masses \tilde{M}_j depend on the parameters M , μ and $\tan\beta$ via Eq.(c18)-(c21) of Ref. [2]. Here we defined $\tan\beta = v_2/v_1$ with v_2 (v_1) being the vev of the Higgs doublet giving up-type (down-type) quark masses, so θ_v in [2] should be substituted by $\pi/2 - \beta$. M is the $SU(2)$ gaugino masses and μ is the coefficient of the $H_1 H_2$ mixing term in the superpotential.

The contribution of Fig.2 to $Z b_R \bar{b}_R$ coupling is given by

$$\begin{aligned} \Delta_R^{(\lambda''_{ij3})} = & -|\lambda''_{ij3}|^2 \frac{f_c}{16\pi^2} \left\{ -B_1(M_b, M_{d^j}, M_{\tilde{u}_R^i}) - B_1(M_b, M_{u^i}, M_{\tilde{d}_R^j}) \right. \\ & + 2 \frac{g_R^{u^i}}{g_R^b} C_{24}(p_b, -k, M_{d^j}, M_{\tilde{u}_R^i}, M_{\tilde{u}_R^i}) + 2 \frac{g_R^{d^j}}{g_R^b} C_{24}(p_b, -k, M_{u^i}, M_{\tilde{d}_R^j}, M_{\tilde{d}_R^j}) \\ & - \frac{g_R^{d^j}}{g_R^b} \left[0.5 - 2C_{24} - M_Z^2(C_{11} - C_{12} + C_{21} - C_{23}) \right. \\ & \left. + \frac{g_L^{d^j}}{g_R^{d^j}} M_{d^j}^2 C_0 \right] (k, -p_{\bar{b}}, M_{d^j}, M_{d^j}, M_{\tilde{u}_R^i}) \\ & - \frac{g_R^{u^i}}{g_R^b} \left[0.5 - 2C_{24} - M_Z^2(C_{11} - C_{12} + C_{21} - C_{23}) \right. \\ & \left. + \frac{g_L^{u^i}}{g_R^{u^i}} M_{u^i}^2 C_0 \right] (k, -p_{\bar{b}}, M_{u^i}, M_{u^i}, M_{\tilde{d}_R^j}) \left. \right\}. \end{aligned} \quad (4.9)$$

Here, for a field f , the left and right-handed couplings are defined by $g_L^f = I_3^f - e_f s_W^2$ and $g_R^f = -e_f s_W^2$ with e_f being the electric charge in unit of e , and $I_3^f = \pm 1/2$ the corresponding third components of the weak isospin. $f_c = 2$ is a color factor.

The contribution of Fig.3 to $Z b_R \bar{b}_R$ coupling is found to be

$$\begin{aligned} \Delta_R^{(\lambda'_{ij3})} = & |\lambda'_{ij3}|^2 \frac{1}{16\pi^2} \sum_{f, \tilde{f}} \left\{ B_1(M_b, M_f, M_{\tilde{f}}) + 2 \frac{g_L^{\tilde{f}}}{g_R^b} C_{24}(p_b, -k, M_f, M_{\tilde{f}}, M_{\tilde{f}}) \right. \\ & - \frac{g_L^f}{g_R^b} \left[0.5 - 2C_{24} - M_Z^2(C_{11} - C_{12} + C_{21} - C_{23}) \right. \\ & \left. + \frac{g_R^f}{g_L^f} M_f^2 C_0 \right] (k, -p_{\bar{b}}, M_f, M_f, M_{\tilde{f}}) \left. \right\}, \end{aligned} \quad (4.10)$$

where the sum is performed over

$$(f, \tilde{f}) = \begin{cases} (d^j, \tilde{\nu}_L^i) \\ (\nu^i, \tilde{d}_L^j) \\ (u^j, \tilde{e}_L^i) \\ (e^i, \tilde{u}_L^j) \end{cases} \quad (4.11)$$

The contribution of Fig.4 to $Z b_L \bar{b}_L$ coupling is given by

$$\Delta_L^{(\lambda'_{i3k})} = |\lambda'_{i3k}|^2 \frac{1}{16\pi^2} \left\{ B_1(M_b, M_{d^k}, M_{\tilde{\nu}^i}) + B_1(M_b, 0, M_{\tilde{d}_R^k}) \right\}$$

$$\begin{aligned}
& -2 \frac{g_L^{\tilde{\nu}^i}}{g_L^b} C_{24}(-p_b, k, M_{d^k}, M_{\tilde{\nu}^i}, M_{\tilde{\nu}^i}) + 2 \frac{g_R^{\tilde{d}^k}}{g_L^b} C_{24}(p_b, -k, 0, M_{\tilde{d}_R^k}, M_{\tilde{d}_R^k}) \\
& - \frac{g_R^{d^k}}{g_L^b} \left[0.5 - 2C_{24} - M_Z^2(C_{11} - C_{12} + C_{21} - C_{23}) \right] (-k, p_{\bar{b}}, M_{d^k}, M_{d^k}, M_{\tilde{\nu}^i}) \\
& + \frac{g_L^{\nu^i}}{g_L^b} \left[0.5 - 2C_{24} - M_Z^2(C_{11} - C_{12} + C_{21} - C_{23}) \right] (k, -p_{\bar{b}}, 0, 0, M_{\tilde{d}_R^k}) \Big\}. \quad (4.12)
\end{aligned}$$

REFERENCES

- [1] For example, see, K. Whisnant, J. M. Yang, B.-L. Young and X. Zhang, Phys. Rev. D **56**, 467 (1997); J. M. Yang and B.-L. Young, Phys. Rev. D **56**, 5907 (1997). G. J. Gounaris, D. T. Papadamou, and F. M. Renard, Z. Phys. C **76**, 333 (1997); G. J. Gounaris, F. M. Renard, and C. Verzegnassi, Phys. Rev. D **52**, 451 (1995); For early references, see, e.g., C. J. C. Burgess and H. J. Schnitzer, Nucl. Phys. **B228**, 454 (1983); C. N. Leung, S. T. Love and S. Rao, Z. Phys. C **31**, 433 (1986); W. Buchmuller and D. Wyler, Nucl. Phys. **B268**, 621 (1986).
- [2] For an introduction to the phenomenology of the MSSM, see H. Haber and G. L. Kane, Phys. Rept. **117**, 75 (1985).
- [3] For some early references on the phenomenology of R -violating supersymmetry, see: L. Hall and M. Suzuki, Nucl. Phys. **B231**, 419 (1984); J. Ellis *et al.*, Phys. Lett. B **150**, 142 (1985); G. Ross and J. Valle, Phys. Lett. B **151**, 375 (1985); S. Dawson, Nucl. Phys. **B261**, 297 (1985); R. Barbieri and A. Masiero, Nucl. Phys. **B267**, 679 (1986); H. Dreiner and G.G. Ross, Nucl. Phys. **B365**, 597 (1991); J. Butterworth and H. Dreiner, Nucl. Phys. **B397**, 3 (1993).
- [4] H1 Collab., C. Adloff *et al.*, DESY 97-024 (1997); ZEUS Collab., J. Breitweg *et al.*, DESY 97-025 (1997).
- [5] Super Kamiokande Collaboration, Y. Fukuda *et al.*, Phys. Rev. Lett. **81**, 1562 (1998); T. Kajita, talk at Neutrino '98, Takayama, Japan, June, 1998; For recent reviews, see, J. M. Conrad, summary talk at ICHEP '98, hep-ex/981109; R. D. Peccei, hep-ph/9906509; H. Robertson, "Neutrino Mass and Oscillations", talk presented at Lepton-Photon'99, the transparencies are available at <http://www-sldnt.slac.stanford.edu/lp99/pdf/33.pdf>.
- [6] For the phenomenology of R -violation in some decays, see: V. Barger, G. F. Giudice and T. Han, Phys. Rev. D **40**, 2978 (1989); K. Agashe and M. Graesser, Phys. Rev. D **54**, 4445 (1996); F. Zwirner, Phys. Lett. B **132**, 103 (1983); R. N. Mohapatra, Phys. Rev. D **34**, 3457 (1986); M. Hirsch, H. Kleingrothaus and S. G. Kovalenko, Phys. Rev. Lett. **75**, 17 (1995); K. S. Babu and R. N. Mohapatra, Phys. Rev. Lett. **75**, 2276 (1995); G. Bhattacharyya and D. Choudhury, Mod. Phys. Lett. A10, 1699 (1995); D. E. Kaplan, hep-ph/9703347; J. Jang, J. K. Kim and J. S. Lee, Phys. Rev. D **55**, 7296 (1997); G. Bhattacharyya and A. Raychaudhuri, Phys. Rev. D **57**, 3837 (1998); J. M. Yang, B.-L. Young and X. Zhang, Phys. Rev. D **58**, 055001 (1998); T.-F. Feng, hep-ph/9806505; S. Bar-Shalom, G. Eilam and A. Soni, hep-ph/9812518.
- [7] For some recent studies of collider phenomenology of R -violation, see: J. Erler, J. L. Feng and N. Polonsky, Phys. Rev. Lett. **78**, 3063 (1997); A. Datta, J. M. Yang, B.-L. Young and X. Zhang, Phys. Rev. D **56**, 3107 (1997); R. J. Oakes, *et al.*, Phys. Rev. D **57**, 534 (1998); J. L. Feng, J. F. Gunion and T. Han, Phys. Rev. D **58**, 071701 (1998); D. K. Ghosh, S. Raychaudhuri and K. Sridhar, Phys. Lett. B **396**, 177 (1997); S. Bar-Shalom, G. Eilam and A. Soni, Phys. Rev. Lett. **80**, 4629 (1998); Phys. Rev. D **59**, 055012 (1999); S. Bar-Shalom, G. Eilam, J. Wudka and A. Soni, Phys. Rev. D **59**, 035010 (1999); B.C. Allanach, H. Dreiner, P. Morawitz and M.D. Williams, Phys. Lett. B **420**, 307 (1998); E. Perez, Y. Sirois and H. Dreiner, hep-ph/9703444.
- [8] For a review of current bounds, see H. Dreiner, hep-ph/9707435, published in *Perspectives on Supersymmetry*, ed. by G. L. Kane; R. Barbier, *et al.*, hep-ph/9810232. G. Bhattacharyya, hep-ph/9709395; P. Roy, hep-ph/9712520.

- [9] T. Appelquist and J. Carazzone, Phys. Rev. D **11**, 2856 (1975).
- [10] G. Bhattacharyya, J. Ellis and K. Sridhar, Mod. Phys. Lett. A10,1583 (1995); G. Bhattacharyya, D. Choudhury and K. Sridhar, Phys. Lett. B **355**, 193 (1995).
- [11] M. Swartz, “Precison Electroweak Physics at the Z”, talk at Lepton-Photon’99, the transparencies are available at <http://www-sldnt.slac.stanford.edu/lp99/pdf/34.pdf>.
- [12] See for example, J. Erler and P. Langacker, hep-ph/9809352; W. Hollik, hep-ph/9811313; W. J. Marciano, hep-ph/9902332.
- [13] A. Joshipura and M. Nowakowski, Phys. Rev. D **51**, 5271 (1995); F. de Campos, M. A. Garcia-Jareno, A. S. Joshipura, J. Rosiek and J. W. F. Valle, Nucl. Phys. **B451**, 3 (1995); V. Barger, M. S. Berger, R. J. N. Phillips, and T. Wöhrmann, Phys. Rev. D **53**, 6407 (1996).
- [14] A. Djouadi, G. Girardi, C. Verzegnassi, W. Hollik and F.M. Renard, Nucl. Phys. **B349**, 48 (1991); M. Boulware and D. Finnell, Phys. Rev. D **44**, 2054 (1991); C.S. Li, J.M. Yang and B.Q. Hu, Commun. Theor. Phys. **20**, 213 (1993).
- [15] J. Ellis and S. Rudaz, Phys. Lett. B **128**, 248 (1983); A. Bouquet, J. Kaplan and C. Savoy, Nucl. Phys. **B262**, 299 (1985).
- [16] B. Brahmachari and P. Roy, Phys. Rev. D **50**, 39 (1994).
- [17] P. Janot, S. Asai and M. Chemarin, presented at the International Europhysics Conference on High Energy Physics, Jerusalem, August 19-26, 1997. To appear in the conference proceedings.
- [18] ALEPH Collaboration, presented at the International Europhysics Conference on High Energy Physics, Jerusalem, August 19-26, 1997. To appear in the conference proceedings.
- [19] D0 Collaboration, Fermilab Pub-96/449-E; Phys. Rev. Lett. **76**, 2222 (1996).
- [20] G. Passarino and M. Veltman, Nucl. Phys. **B160**, 151 (1979).

TABLES

TABLE I. The 1σ upper limits on B -violating top quark couplings λ''_{3j3} from R_b for scenario A ($M = 250$ GeV, $\mu = -100$ GeV) and scenario B ($M = 100$ GeV, $\mu = -250$ GeV). The 2σ upper limits are weaker than the perturbative unitarity bound of 1.25 and thus not listed here.

sfermion mass (GeV)	Scenario A		Scenario B	
	$\tan \beta = 2$	$\tan \beta = 30$	$\tan \beta = 2$	$\tan \beta = 30$
100	1.23	1.18	1.07	0.87
200	1.30	1.26	1.06	0.82
300	1.39	1.36	1.12	0.86
400	1.48	1.45	1.19	0.93
500	1.57	1.55	1.27	1.02
600	1.65	1.64	1.36	1.12
700	1.77	1.73	1.45	1.23
800	1.72	1.89	1.54	1.33
900	1.91	1.90	1.63	1.43
1000	2.01	2.00	1.73	1.54

TABLE II. The 1σ (2σ) upper limits on B -violating top quark couplings λ''_{3j3} from R_ℓ for scenario A ($M = 250$ GeV, $\mu = -100$ GeV) and scenario B ($M = 100$ GeV, $\mu = -250$ GeV). These bounds are also applied to λ''_{3jk} if all sfermions have the same mass.

sfermion mass (GeV)	Scenario A		Scenario B	
	$\tan \beta = 2$	$\tan \beta = 30$	$\tan \beta = 2$	$\tan \beta = 30$
100	0.75(1.14)	0.72(1.12)	0.65(1.08)	0.53(1.01)
200	0.79(1.30)	0.77(1.29)	0.65(1.22)	0.51(1.15)
300	0.85(1.49)	0.83(1.48)	0.69(1.40)	0.54(1.34)
400	0.91(1.68)	0.89(1.67)	0.74(1.59)	0.59(1.53)
500	0.96(1.86)	0.95(1.86)	0.79(1.78)	0.65(1.72)
600	1.02(2.04)	1.01(2.04)	0.85(1.96)	0.71(1.91)
700	1.09(2.24)	1.07(2.23)	0.91(2.15)	0.78(2.10)
800	1.07(2.38)	1.17(2.42)	0.97(2.33)	0.84(2.29)
900	1.19(2.57)	1.18(2.57)	1.02(2.50)	0.91(2.46)
1000	1.25(2.75)	1.24(2.75)	1.09(2.69)	0.98(2.64)

TABLE III. The 1σ (2σ) upper limits on L -violating top quark couplings λ'_{13k} from R_e for scenario A ($M = 250$ GeV, $\mu = -100$ GeV) and scenario B ($M = 100$ GeV, $\mu = -250$ GeV).

sfermion mass (GeV)	Scenario A		Scenario B	
	$\tan \beta = 2$	$\tan \beta = 30$	$\tan \beta = 2$	$\tan \beta = 30$
100	0.72(0.89)	0.72(0.90)	0.73(0.91)	0.75(0.92)
200	0.87(1.08)	0.87(1.08)	0.89(1.10)	0.91(1.11)
300	1.04(1.29)	1.05(1.29)	1.06(1.30)	1.08(1.32)
400	1.21(1.49)	1.22(1.50)	1.23(1.51)	1.25(1.52)
500	1.38(1.70)	1.38(1.70)	1.40(1.71)	1.41(1.72)
600	1.54(1.90)	1.55(1.90)	1.56(1.91)	1.57(1.92)
700	1.70(2.09)	1.71(2.09)	1.72(2.10)	1.73(2.11)
800	1.87(2.29)	1.86(2.28)	1.88(2.30)	1.89(2.30)
900	2.02(2.47)	2.02(2.47)	2.03(2.49)	2.04(2.49)
1000	2.17(2.66)	2.17(2.66)	2.19(2.67)	2.20(2.68)

TABLE IV. The 1σ (2σ) upper limits on L -violating top quark couplings λ'_{23k} from R_μ for scenario A ($M = 250$ GeV, $\mu = -100$ GeV) and scenario B ($M = 100$ GeV, $\mu = -250$ GeV).

sfermion mass (GeV)	Scenario A		Scenario B	
	$\tan \beta = 2$	$\tan \beta = 30$	$\tan \beta = 2$	$\tan \beta = 30$
100	0.58(0.74)	0.58(0.74)	0.60(0.75)	0.62(0.77)
200	0.71(0.89)	0.71(0.90)	0.73(0.91)	0.75(0.93)
300	0.86(1.07)	0.86(1.07)	0.88(1.09)	0.90(1.11)
400	1.00(1.25)	1.00(1.25)	1.02(1.27)	1.04(1.28)
500	1.14(1.42)	1.14(1.42)	1.16(1.44)	1.18(1.45)
600	1.28(1.58)	1.28(1.59)	1.30(1.60)	1.31(1.61)
700	1.41(1.75)	1.41(1.75)	1.43(1.77)	1.45(1.78)
800	1.55(1.92)	1.54(1.91)	1.57(1.93)	1.58(1.94)
900	1.68(2.07)	1.68(2.07)	1.70(2.09)	1.71(2.09)
1000	1.80(2.23)	1.81(2.23)	1.82(2.24)	1.83(2.25)

TABLE V. The 1σ (2σ) upper limits on L -violating top quark couplings λ'_{33k} from R_τ for scenario A ($M = 250$ GeV, $\mu = -100$ GeV) and scenario B ($M = 100$ GeV, $\mu = -250$ GeV).

sfermion mass (GeV)	Scenario A		Scenario B	
	$\tan \beta = 2$	$\tan \beta = 30$	$\tan \beta = 2$	$\tan \beta = 30$
100	0.16(0.54)	0.18(0.55)	0.22(0.56)	0.27(0.58)
200	0.26(0.67)	0.27(0.67)	0.32(0.69)	0.36(0.71)
300	0.35(0.81)	0.36(0.81)	0.41(0.83)	0.44(0.85)
400	0.43(0.94)	0.44(0.95)	0.49(0.97)	0.52(0.99)
500	0.51(1.08)	0.51(1.08)	0.56(1.10)	0.59(1.12)
600	0.58(1.21)	0.59(1.21)	0.63(1.23)	0.66(1.25)
700	0.65(1.34)	0.66(1.34)	0.70(1.36)	0.73(1.37)
800	0.74(1.47)	0.72(1.46)	0.77(1.49)	0.79(1.50)
900	0.80(1.59)	0.80(1.59)	0.83(1.61)	0.86(1.62)
1000	0.86(1.71)	0.86(1.71)	0.90(1.73)	0.92(1.74)

TABLE VI. A summary of updated current bounds on R -violating top quark Yukawa couplings for slepton mass and squark mass of 100 GeV.

Top Quark R-violating Couplings	Limits	Sources
λ'_{131}	0.035	APV, 2σ
λ'_{132}	0.75(0.92)	R_e at LEP, 1σ (2σ)
λ'_{133}	0.0007	ν_e -mass, 1σ
λ'_{231}	0.22	ν_μ scatter, 2σ
$\lambda'_{232}, \lambda'_{233}$	0.62(0.77)	R_μ at LEP, 1σ (2σ)
$\lambda'_{331}, \lambda'_{332}, \lambda'_{333}$	0.27(0.58)	R_τ at LEP, 1σ (2σ)
$\lambda''_{312}, \lambda''_{313}, \lambda''_{323}$	0.75(1.14)	R_ℓ at LEP, 1σ (2σ)

FIGURES

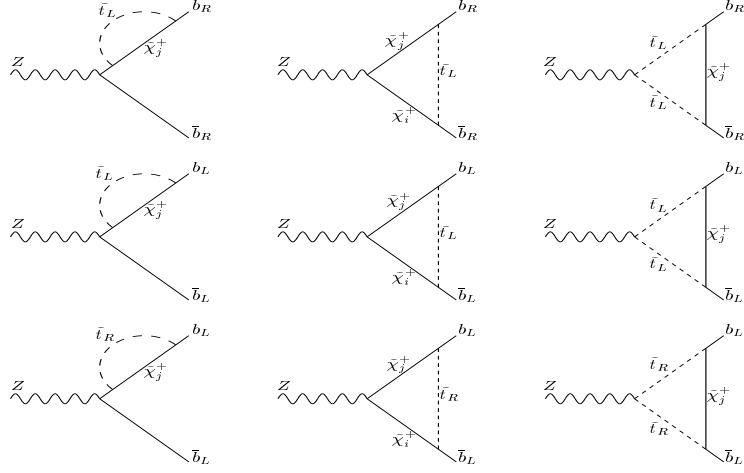


FIG. 1. Feynman diagrams of chargino-stop loops which contribute to $Zb\bar{b}$ vertex.

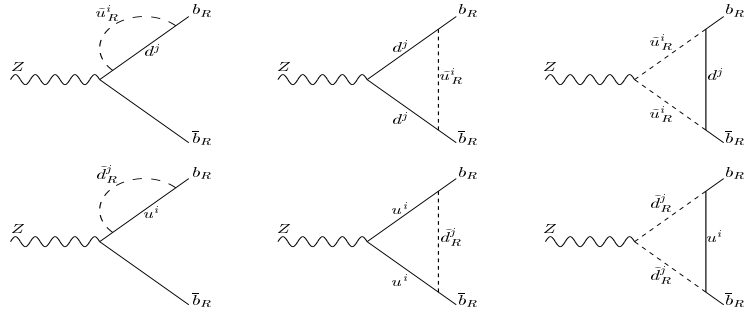


FIG. 2. Feynman diagrams for the B -violating λ''_{ij3} contributions to $Zb_R\bar{b}_R$ vertex. i and j are flavor indices, with $i = 1, 2$ or 3 and $j = 1$ or 2 .

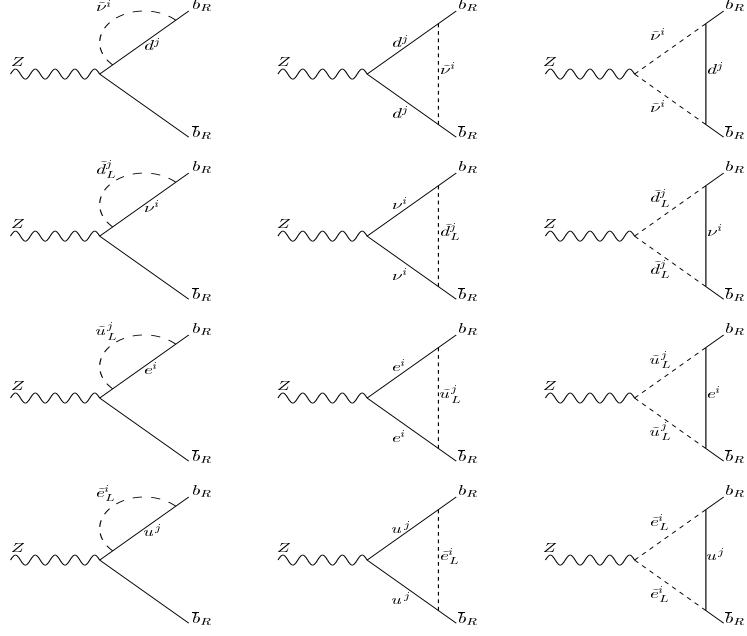


FIG. 3. Feynman diagrams for the L -violating λ'_{ij3} contributions to $Zb_R\bar{b}_R$ vertex. i and j are flavor indices.

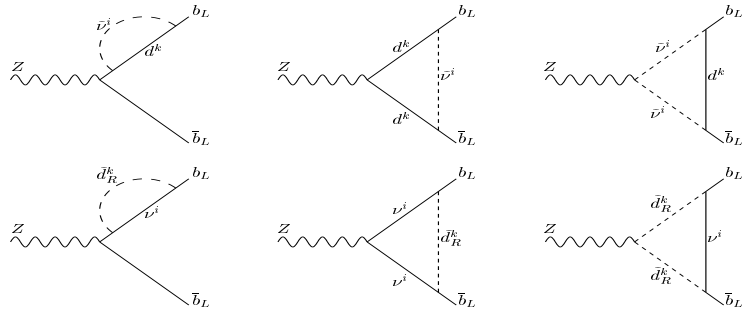


FIG. 4. Feynman diagrams for the L -violating λ'_{i3k} contributions to $Zb_L\bar{b}_L$ vertex. i and k are flavor indices.

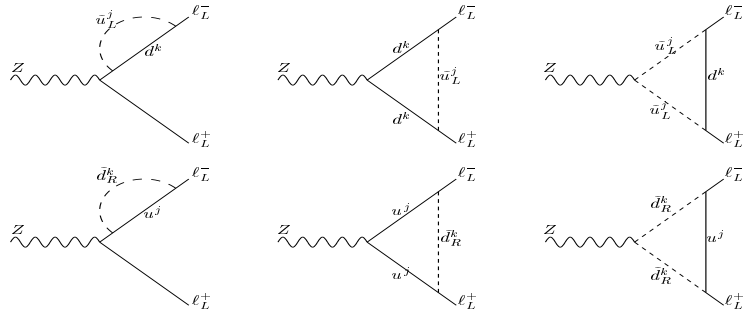


FIG. 5. Feynman diagrams for the L -violating λ'_{i3k} contributions to left-handed $Z\ell_L\ell_L$ vertex. i and k are flavor indices.

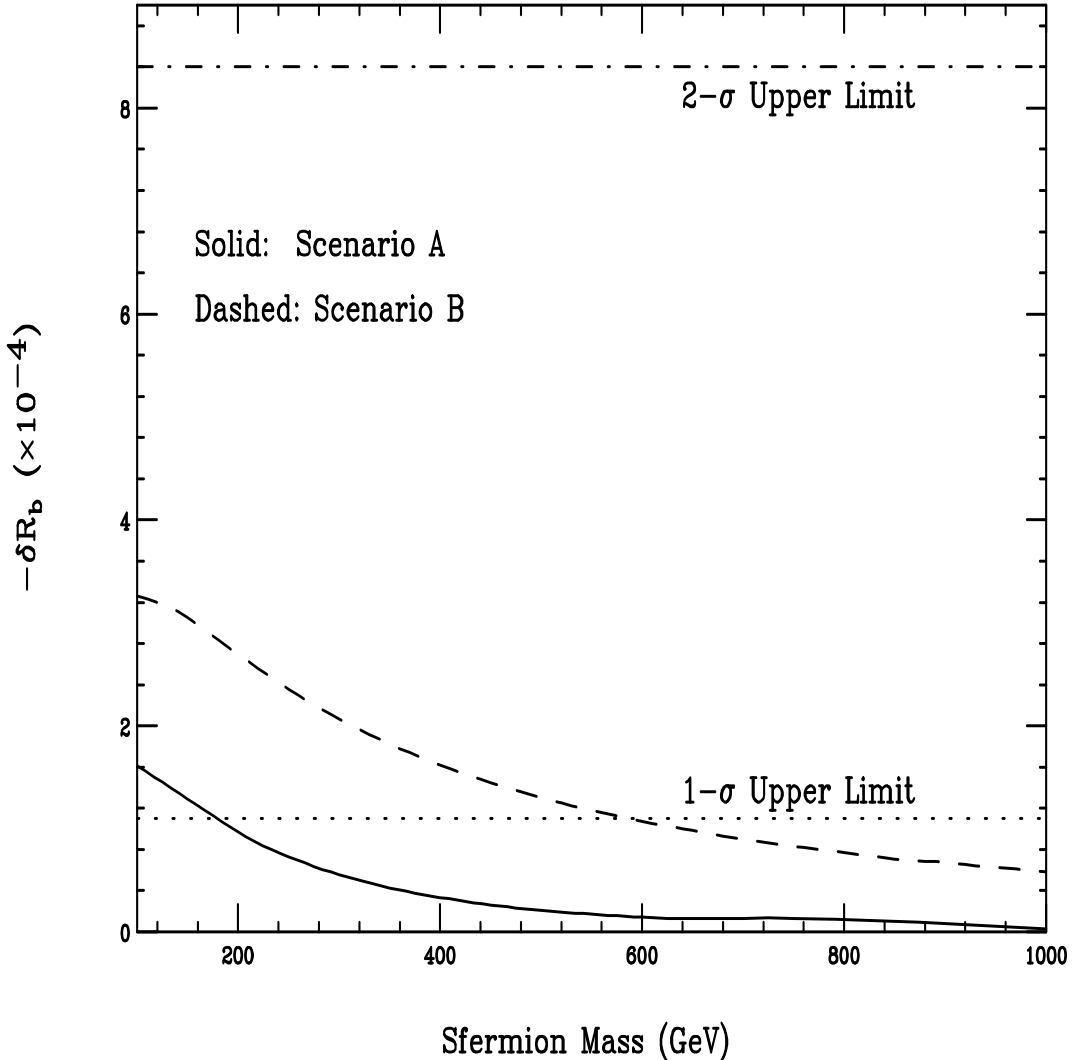


FIG. 6. δR_b in the presence of $\lambda_{3j3}'' = 1.25$ versus sfermion mass for scenario A ($M = 250$ GeV, $\mu = -100$ GeV) and scenario B ($M = 100$ GeV, $\mu = -250$ GeV).

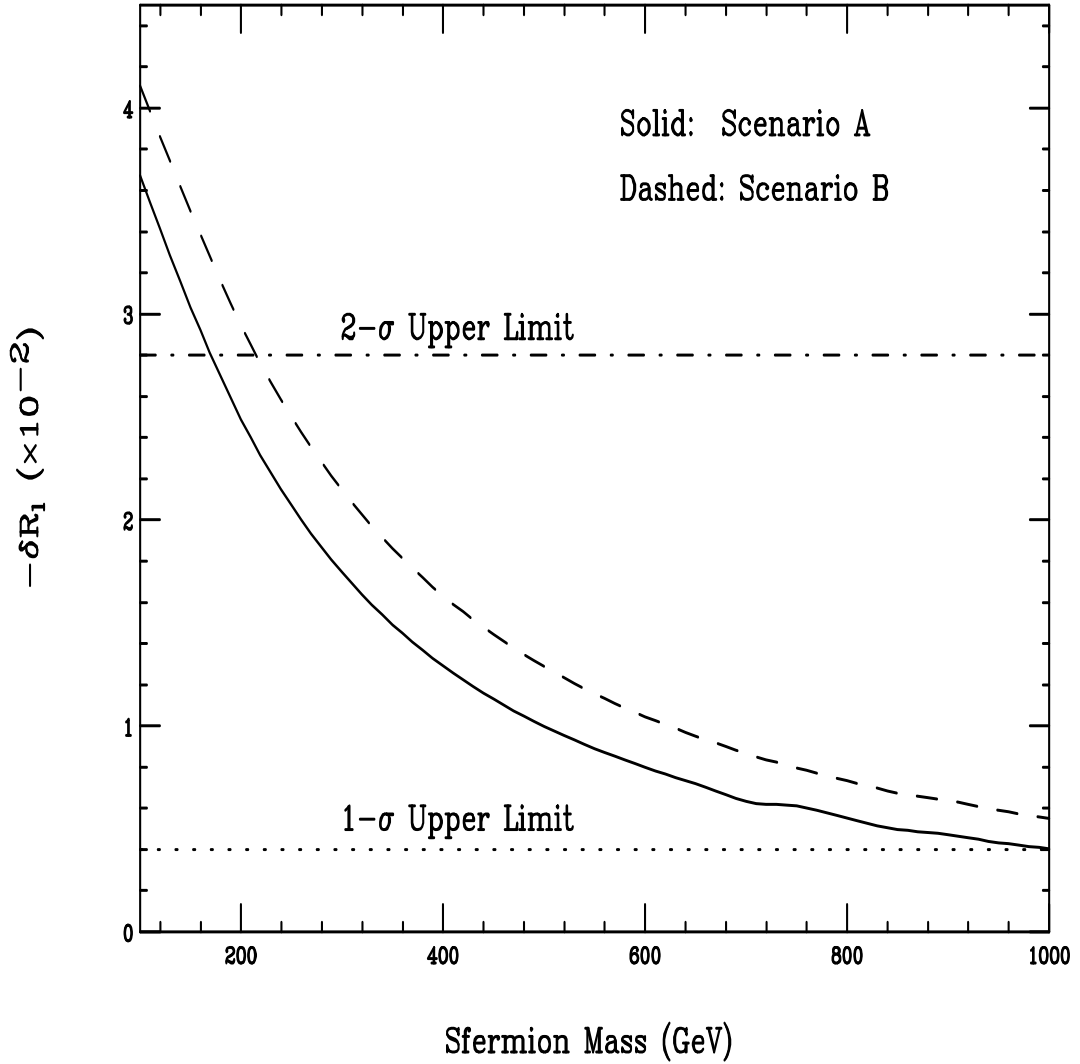


FIG. 7. δR_ℓ in the presence of $\lambda''_{3j3} = 1.25$ versus sfermion mass for scenario A ($M = 250$ GeV, $\mu = -100$ GeV) and scenario B ($M = 100$ GeV, $\mu = -250$ GeV).

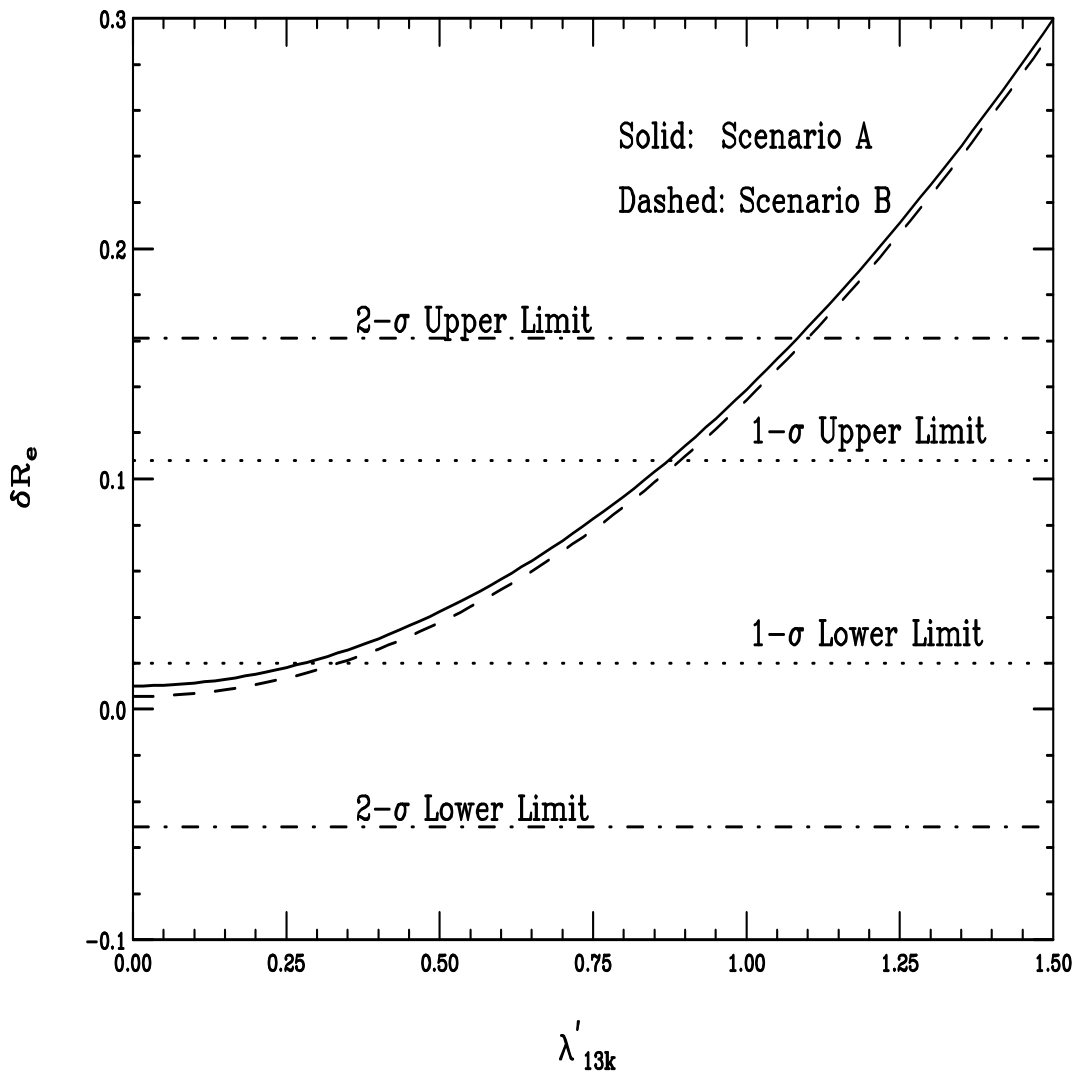


FIG. 8. δR_e versus λ'_{13k} for versus sfermion mass of 200 GeV, under scenario A ($M = 250$ GeV, $\mu = -100$ GeV) and scenario B ($M = 100$ GeV, $\mu = -250$ GeV).

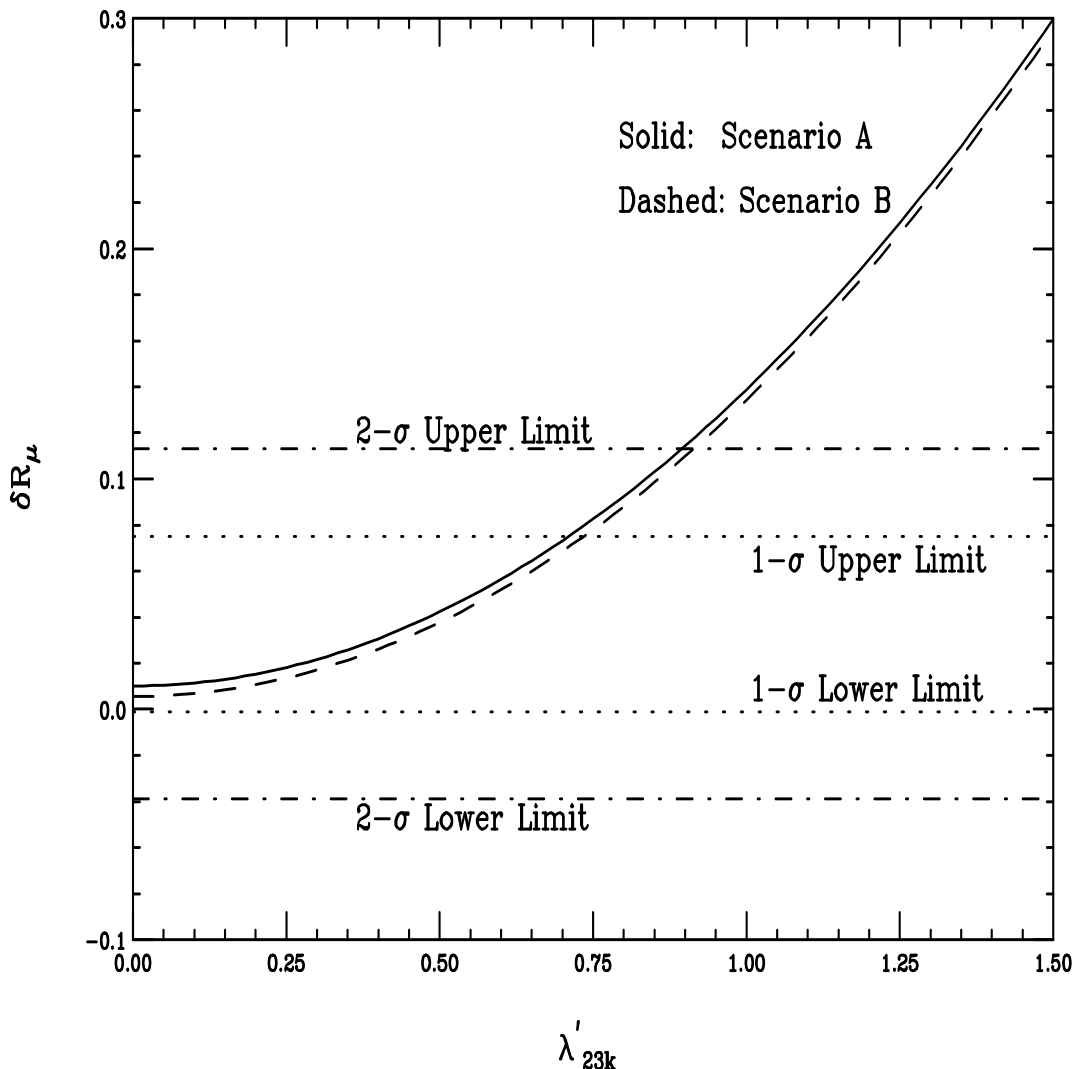


FIG. 9. Same as Fig. 8, but for δR_μ versus λ'_{23k} .

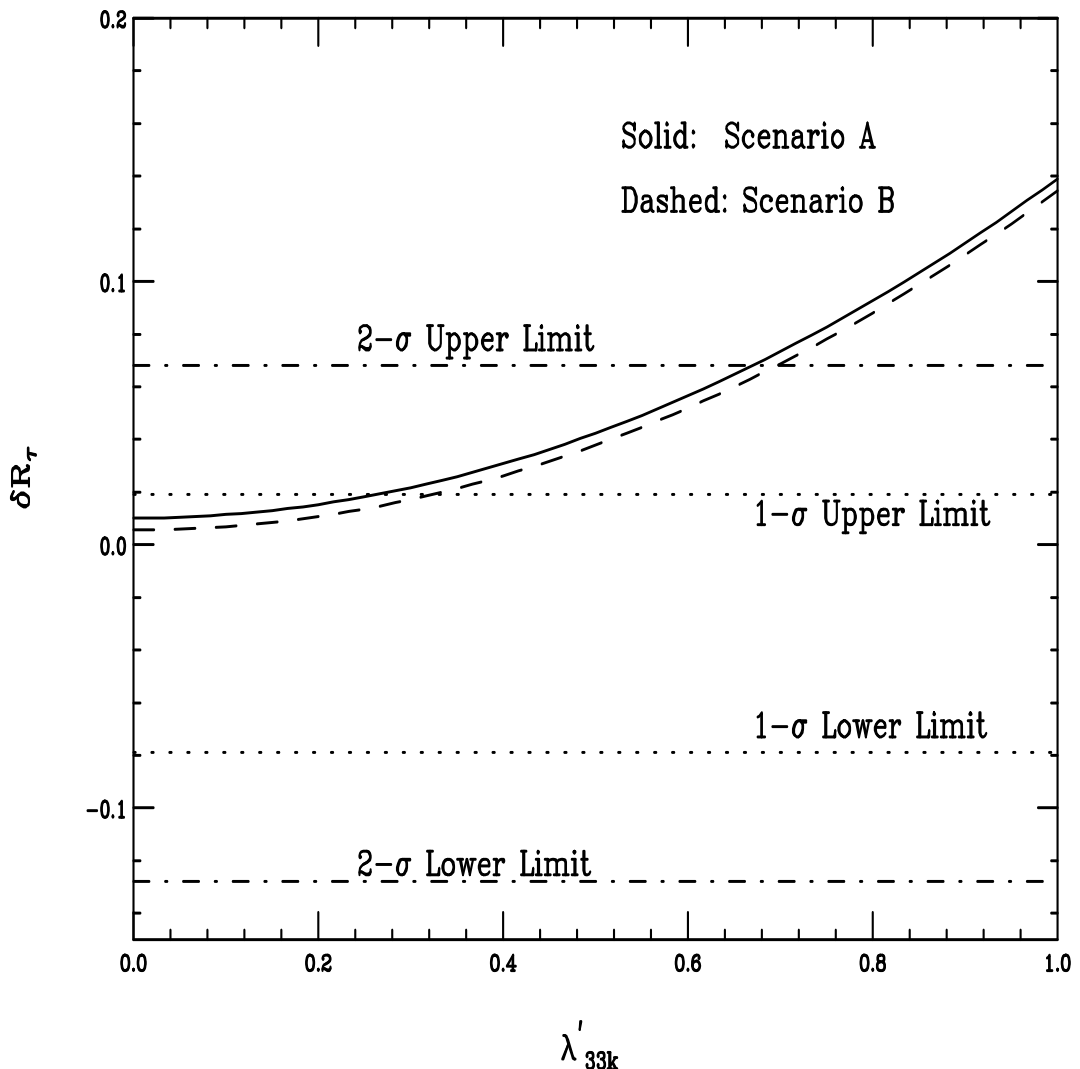


FIG. 10. Same as Fig. 8, but for δR_τ versus λ'_{33k} .